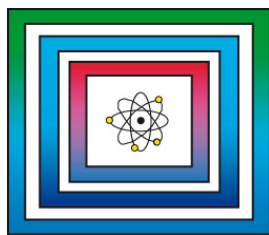# R+D
Radioactive Waste Repository

9Y3214100000

Triaxial
Compaction Test
TK-031

Evaluation Report

Hannover, August 2013

FEDERAL INSTITUTE FOR GEOSCIENCES
AND NATURAL RESOURCES
HANNOVER

R+D Radioactive Waste Repository

THM Geotechnical barriers

Triaxial Compaction Test TK-031

Evaluation Report

Author:	Stührenberg, Dieter, Dr.

Order number:	9Y3214100000
Reference no:	B3.4/B50112-09/2015-0002/001
Date:	23.08.2013

By order:

signed V. Bräuer

Dr. V. Bräuer (Head of Department B3), Project leader Final Disposal

R & D Radioactive Waste Repository
STÜHRENBERG, D.(2013): Triaxial Compaction Test TK-031
Evaluation Report; Hannover (BGR)

Page 2 of 33

Table of contents
Page

Number of pages: 33

R & D Radioactive Waste Repository
STÜHRENBERG, D.(2013): Triaxial Compaction Test TK-031
Evaluation Report; Hannover (BGR)

Page 3 of 33

Abstract

Author: Stührenberg, Dieter, Dr.

Title: Triaxial Compaction Test TK-031

Subject terms: compaction, crushed salt, geomechanics,
                                               laboratory investigations, residual porosity

As part of the REPOPERM project (Residual Porosity and Permeability of Compacted Crushed Salt Backfill in a High Level Radioactive Waste Repository) a triaxial compaction test with the code number TK-031 was carried out using crushed salt material z2SP from the Asse mine ("Speisesalz", w ≈ 0.05 wt.-%) of grain size distribution curve "DEBORA" (d ≤ 8.0 mm). This triaxial test was undertaken to determine the compaction rates affecting the sample under site-specific relevant stresses until the sample enters the residual porosity range. Differences were revealed on the basis of comparisons with the results of displacement controlled odometer tests. The TK-031 test did not confirm the strong decline in compaction rates in the residual porosity range suggested by the odometer tests, which originally suggested that the in situ duration of the compaction process would be unacceptably long.

The results of test TK-031 were extrapolated to estimate the material behaviour beyond the test period. The results of this extrapolation indicated that a void ratio of 0.2 % would be reached after around 5 years.

R & D Radioactive Waste Repository
STÜHRENBERG, D.(2013): Triaxial Compaction Test TK-031
Evaluation Report; Hannover (BGR)

Page 4 of 33

1 Reasons for carrying out the test and the objective

An understanding of the three-dimensional stress state of crushed salt is required to describe the time-dependent compaction behaviour of crushed salt using material laws with variable parameters. This cannot be determined to the necessary degree of accuracy by odometer tests. To supplement and independently assess the results of the displacement controlled compaction by odometer measurements, triaxial compaction tests were undertaken with known compaction forces, axial force and confining pressure. The parameters to be determined by this test are the void ratio and the compaction rate. During the test, the sample was to be compacted as far as possible, but without exceeding the maximum formation pressure expected in situ.

2 Test apparatus and test procedure

2.1 Precompaction of the test samples

The triaxial tests are carried out on odometrically (uniaxial) pre-compacted crushed salt material (void ratio e ≈ 0.2) so that the samples are manageable when being installed in the triaxial cell, and so that the initial void ratio can be determined from a sufficiently accurate cylinder geometry. It is still possible, however, that air pockets could be trapped behind the sleeve which is required around the outside of the sample and which could falsely suggest the existence of sample compaction as the pressure is initially built up in the triaxial test apparatus.

The pre-compaction of the loose crushed salt takes place in line with the odometer principle in a steel cylinder consisting of four quarter sleeves with an internal diameter of 10.0 cm. The quarter sleeves are removed when pre-compaction has been completed so that the sample can be extracted without damaging it. To ensure that the compaction is as homogenous as possible, the sample is compacted from both sides by reversing the cylinder and the sample when the compression die has moved around 50 % of its ultimate stroke.

2.2   Triaxial compaction with volume measurement

The pre-compacted crushed salt test specimen – TK-031 in this case – is encased in a Teflon and rubber sleeve and installed in the M6 triaxial cell at BGR. Fig. 1 shows a sketch of the apparatus without the frame of the machine and the main cylinder for axial force F_1. The force is applied to the sample axially via piston force F_1 and the lateral confining pressure ρ_i (Kármán principle).

The whole of the compacted volume is determined with the help of the volume of air ΔV displaced from the compacted sample. A sinter plate (fuse disk) and a pressure plate with drilled holes are positioned on the upper axial face of the sample. This feeds the displaced air into a reservoir filled with a liquid which is connected to two burettes with different capacities. The amount of air displaced can be measured from the rise in the fluid level in the burette which can then be used to determine the compaction volume ΔV after carrying out the necessary corrections (see below).
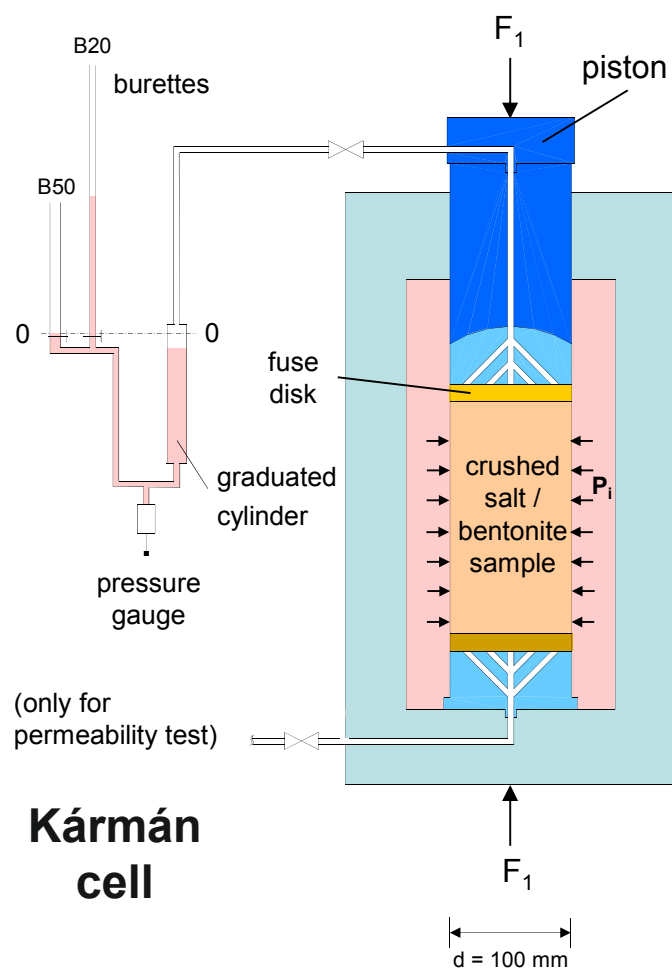

Fig. 1:   Sketch of the triaxial test apparatus M6 (TRE-2001)

R & D Radioactive Waste Repository
Sᴛüʜʀᴇɴʙᴇʀɢ, D.(2013): Triaxial Compaction Test TK-031
Evaluation Report; Hannover (BGR)

Page 6 of 33

The volume measurement apparatus was developed by BGR in 1994 and has undergone several modifications and improvements since this date, e.g. by installing gas-tight connections and computer-supported registration of the pressure in the measurement columns. The general methodology and the calibration are described in detail in Sᴛüʜʀᴇɴʙᴇʀɢ & Zʜᴀɴɢ (1995). Critical aspects are the geometrical conditions of the measurement system and the compressibility of the air in the sample and in the piping. Moreover, the level of liquid in the open system is affected by fluctuations in atmospheric pressure, temperature changes, and gradual evaporation of the measurement liquid during the course of longer testing periods.

Interventions in the continuous series of measurements occurs during "venting" of the activated measurement burette when the fluid level has to be lowered to prevent the capacity of the burette from being exceeded – this is done by reducing the amount of air in the system and lowering the internal pressure. Whenever possible, this intervention in the test is undertaken during the testing period with constant loading and continuous compaction to ensure that it is possible to differentiate between the sample-related changes and the measuring-system-related changes. In the case of highly compacted specimens, it can take several hours for equilibrium to be reached between the pore pressure in the specimen and the pressure in the connected system. The effect of the pressure compensation during venting is removed from the registered $\Delta V/\Delta t$ curves. Moreover, it is also assumed that internal changes in pressure of only a few millibars will not have any significant influence on the compaction behaviour of the crushed salt specimen under external loads in the order of 10 to 20 MPa.

The ratio of volume reduction ΔV to oil level rise ΔV_f for a burette filling was determined in good approximation to be linear ($\Delta V/\Delta V_f = C_3$) on the basis of compaction tests in an odometer-like cell (uniaxial parameters) with defined geometrical conditions and specimen volumes. Fig. 2 shows the results of the AVOL-B110 calibration tests (room temperature, T = 29 – 33 °C, blue) and AVOL-B111 (T ≈ 50 °C, magenta). The factors dependent on the air volume in the measurement system reduce with increasing compaction. These results can be transferred to the triaxial test because of the analogous geometrical conditions, even though the amount of scatter increases significantly in the relevant void ratio range between 0.2 > e > 0.07. The main reference points for modifications undertaken for the triaxial test are therefore the initial and final condition parameters directly measured from the crushed salt specimen. These were also used in test TK-031 to adjust the C_3 values as part of the final evaluation. The resulting red curve in Fig. 2 is explained in Chapter 3.5.

The fluctuations in atmospheric pressure ΔP_a measured in the triaxial test and clearly visible in the plot showing the height of the fluid level, are multiplied by an empirically determined factor and superimposed on the measured values.

R & D Radioactive Waste Repository
STÜHRENBERG, D.(2013): Triaxial Compaction Test TK-031
Evaluation Report; Hannover (BGR)
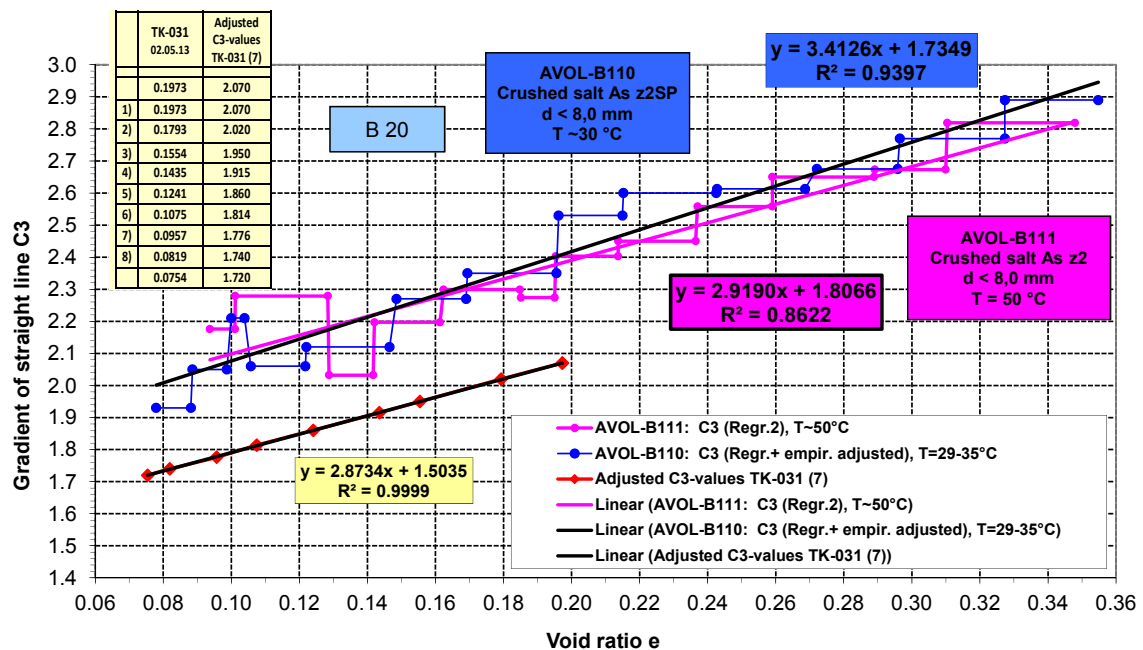
Page 7 of 33

Fig. 2:   Determination of the C_3 values from calibration tests and adjustments for TK-031

The results can be corrected for temperature fluctuations in the same way, although those usually only occur if problems arise in the heatable triaxial cell where the usual value is $\Delta TZ \leq 1.0\ °C$ or in air-conditioned rooms where $\Delta TR \leq \pm\ 1.0\ °C$ under usual circumstances. Zero point correction of the measured value may be necessary at the start of the test if the sleeve around the specimen and the O-ring between the piston and the pressure plate still contain air inclusions arising from the technical set-up (cf. Chapter 3.5), and which must not be confused with the sample porosity.

The axial sample ΔH is determined outside of the cell by an inductive displacement transducer used to record the movement of the piston. The measured value ΔH must be corrected to compensate for the compression of the O-ring between the pressure plate and the axial piston (see above) and any compression which may arise in the sinter plate which is installed to ensure the unhindered escape of the volume of air displaced from the sample.

2.3   Specified values, measurement and definition parameters

The specified parameters in the axial direction critical for the test programme are the constant vertical stress σ1 and the loading speed also selected as constant for the load increases. These are related to the changeable current specimen cross-section A which cannot be measured directly but can only be determined from the overall deformation and/or compaction (see below).

The force F_1 or force rate $\dot{F}_1$ to be applied by the machine must be converted accordingly. This conversion is undertaken in the evaluation independent of the process control with the necessary default correction values.

$$\sigma_1 = \frac{F_1}{A} \tag{1}$$

$$\dot{\sigma}_1 = \frac{\dot{F}_1}{A} - \frac{F_1 \cdot \dot{A}}{A^2} \approx \frac{\dot{F}_1}{A} \tag{2}$$

The radial stress σ_3 is identical to the cell oil pressure p_i:

$$\sigma_3 = p_i \tag{3}$$

The other stress parameters for cylindrical specimens are defined as follows:

Mean stress (pressure positive): $\quad \sigma_m = (\sigma_1 + 2\sigma_3)/3 \tag{4}$

Deviatoric stress: $\quad \Delta\sigma = (\sigma_1 - \sigma_3) \tag{5}$

The strain or compaction parameters are determined from the measured change in height ΔH and the displaced internal volume ΔV of the sample (see below). The reference parameter is the installation state (technical strain level). The axial strain ε_1 is therefore determined from the initial height H_0 and the current specimen height H, whereby H is determined from the initial height H_0 and the measured change in height ΔH:

$$\varepsilon_1 = \frac{\Delta H}{H_0} = \frac{H_0 - H}{H_0} \tag{6}$$

The volumetric strain ε_v is defined positively as compaction:

$$\varepsilon_v = \frac{\Delta V}{V_0} = \frac{V_0 - V}{V_0} \tag{7}$$

If the cylindrical specimen is assumed to maintain its shape during the compaction, the diameter of the specimen D and the radial strain $\varepsilon_2 = \varepsilon_3$ are calculated as follows:

$$D = \sqrt{\frac{4V}{\pi H}} \tag{8}$$

and

$$\varepsilon_3 = \frac{\Delta D}{D_0} = \frac{D_0 - D}{D_0} \tag{9}$$

The comparative parameter for the state of compaction is the void ratio:

$$e = \frac{V - V_S}{V_S} = \frac{V_P}{V_S} = \frac{\rho_S}{\rho_{Sgr}} - 1 \tag{10}$$

where

$$\rho_{Sgr} = \frac{m}{V} \tag{11}$$

and:

V_S = volume of the specimen after complete compaction (rock salt)

V_P = pore volume of the sample

ρ_S = rock salt density

ρ_{Sgr} = density of the crushed salt

m = mass of the crushed salt (weight of the sample)

Because the solid volume of the unconsolidated specimen is unknown, the calculations are carried out using the density determined from analogous rock salt material.

The state of compaction is often measured in terms of porosity:

$$\Phi = \frac{V - V_S}{V} = \frac{V_P}{V} = 1 - \frac{\rho_{Sgr}}{\rho_S} \tag{12}$$

With the conversion:

$$\Phi = \frac{e}{1 + e} \tag{13}$$

$$e = \frac{\Phi}{1 - \Phi} \tag{14}$$

R & D Radioactive Waste Repository
STÜHRENBERG, D.(2013): Triaxial Compaction Test TK-031
Evaluation Report; Hannover (BGR)

Page 10 of 33

3   Material, test procedure, results and evaluation

3.1   Test material and solid density

The crushed salt used in test VK-020/TK-031 originated from the Asse mine, and specifically from the special facies "Speisesalz" (As z2SP) of the Älteres Steinsalz z2. According to mineral analysis undertaken by BGR/LBEG, it consists of over 99 % halite (DOHRMANN, 2010). After BRAITSCH (1962) and KRÖHN et al. (2009), Section 4.3.2, the following is used as the calculated solid density in a "dry" state:

$$\rho_S^{tr} = 2.169 \text{ g/cm}^3 \tag{15}$$

A sieve curve of d_{max} = 8.0 mm was selected in accordance with the sieve underflow line for borehole backfill stipulated in KRÖHN et al. (2009), Fig. 2.1 ("DEBORA/REPOPERM project").

6 samples of the crushed salt mixture made available for pre-compaction (30, 50 and 100 g) were dried in a thermal cabinet at 105 °C in September 2011. The moisture contents lay between 0.02 and 0.1 wt-%. A mean value of w = 0.05 wt-% was assumed. This gives the following for crushed salt sample VK-020/TK-031 to calculate the void ratio e in a "moist" state:

$$\rho_S^{f} = 2.169*1.0005 = 2.170 \text{ g/cm}^3 \tag{16}$$

3.2   Pre-compaction test VK-020

The crushed salt z2SP, d_{max} = 8.0 mm, intended for triaxial test TK-031 was filled into the pre-compaction cylinder in 5 layers (d = 100 mm). The aggregate mass was 2800.6 g. This was then odometrically pre-compacted as test VK-020 in 2 x 8 days at a speed of ṡ = 0.136 mm/h (approx. $1.5 * 10^{-7}$ s^{-1}). The initial void ratio was 0.518 based on the initial height of 24.9 cm and the defined rock salt density ρ_S^{f} = 2.170 g/cm². The sample was calculated to contain 1.4 g water. The continuously growing axial stress, including the inseparable frictional forces, totalled 29 MPa at the end of the pre-compaction test. After removal from the apparatus, the now relatively consolidated crushed salt cylinder had a height of 19.65 cm. Its weight of 2797.7 g was 0.1 % smaller than the aggregate mass of the crushed salt filled into the cylinder.

R & D Radioactive Waste Repository
Stührenberg, D.(2013): Triaxial Compaction Test TK-031
Evaluation Report; Hannover (BGR)

Page 11 of 33

3.3 Initial values and overview TK-031

The pre-compacted crushed salt test specimen was surrounded by a Teflon and rubber sleeve and installed in the M6 triaxial cell (14.11.2011). The following initial values were recorded: diameter: D = 100 mm, height: H = 196.5 mm, mass: m = 2797.7 g, initial void ratio: e_0 = 0.1973. The specimen volume of 1543 cm^3 was calculated to consist of 1289 cm^3 rock salt and 254 cm^3 pore space.

Figure 3 shows an overview of the course of the test over time. Figure 3 shows the stress components σ_1 and σ_3 applied to the specimen, the mean stress σm, the difference in the components and their percentage proportions related to σ_3. The slightly higher axial stress is required for mechanical-technical reasons to ensure a solid connection between the compression die and the upper pressure plate. The void ratio e calculated from the measurements with respect to the secondary axis is shown as a result of the evaluation described in Chapter 3.5.
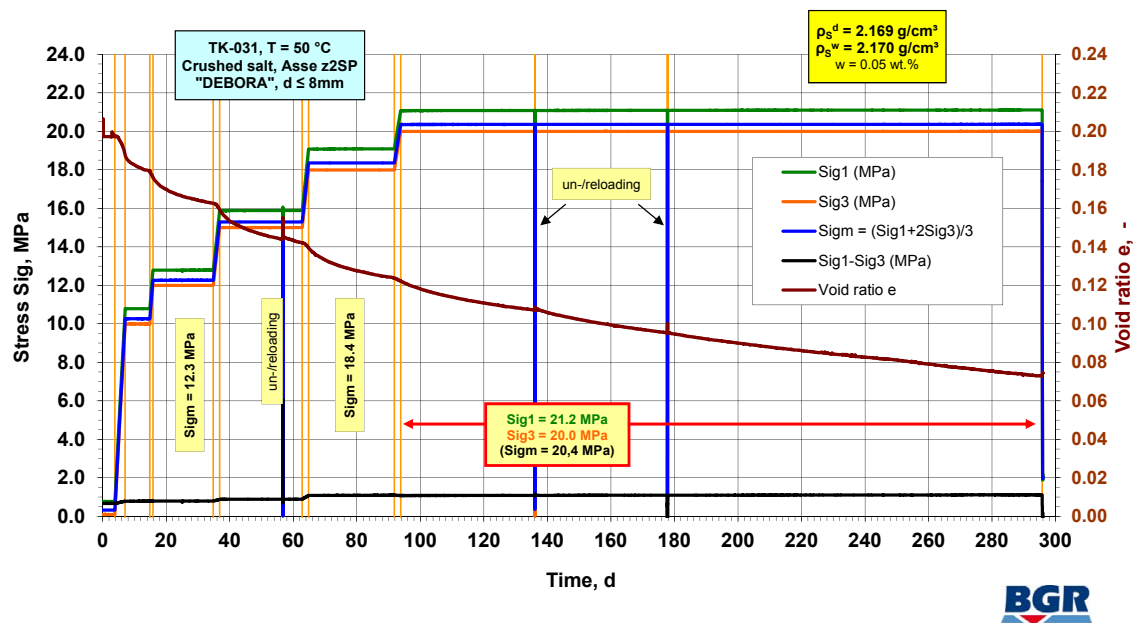

Fig. 3: TK-031- Change of stresses and compaction over time

The test run included 5 different stress phases consisting of loading (load increases) and the associated creep compaction phases:

$\sigma_1/\sigma_3/\sigma_m$ = 10.8/10.0/10.3 MPa; 12.8/12.0/12.3 MPa; 15.9/15.0/15.3 MPa; 19.1/18.0/18.4 MPa und 21.1/20.0/20.4 MPa.

Figure 4 shows the volumetric strain ε_v determined from the volume measurements according to eq. (7), the strain ε_1 determined from the axial deformation in accordance with eq. (6), and the radial strain ε_3 on the primary axis determined in accordance

R & D Radioactive Waste Repository
STÜHRENBERG, D.(2013): Triaxial Compaction Test TK-031
Evaluation Report; Hannover (BGR)

Page 12 of 33

with eq. (9). The temporal extrapolations of these parameters as strain rates are shown with respect to the secondary axis. Because of the measurement accuracy achievable for these volume measurements, the oscillation of the strain rates is strongly dependent on the selected time interval. For calculation purposes, the total number of measurement times of 4079 was reduced to 152. The points on the plots refer to the middle of the time interval selected in each case. The void ratios are given for the beginning of each new loading phase and at some of the other test times.
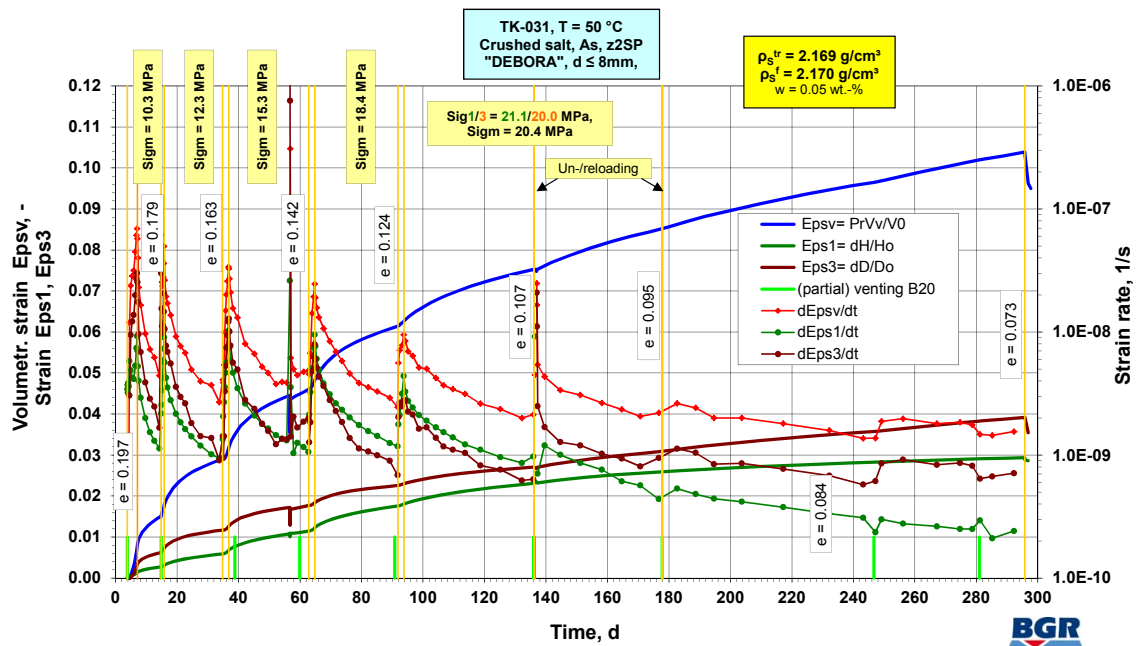
Fig. 4:   Strain and strain rates during test TK-031

Figure 5 visualises the determined void ratios as a function of the applied mean stress σ$_m$. It is possible to clearly differentiate between the 5 loading phases (load increases), the creep compaction phases with constant external stresses, the 3 brief pressure release phases during the test, and the void ratio correction undertaken because of the sleeve surrounding the specimen (see Chapter 3.5).
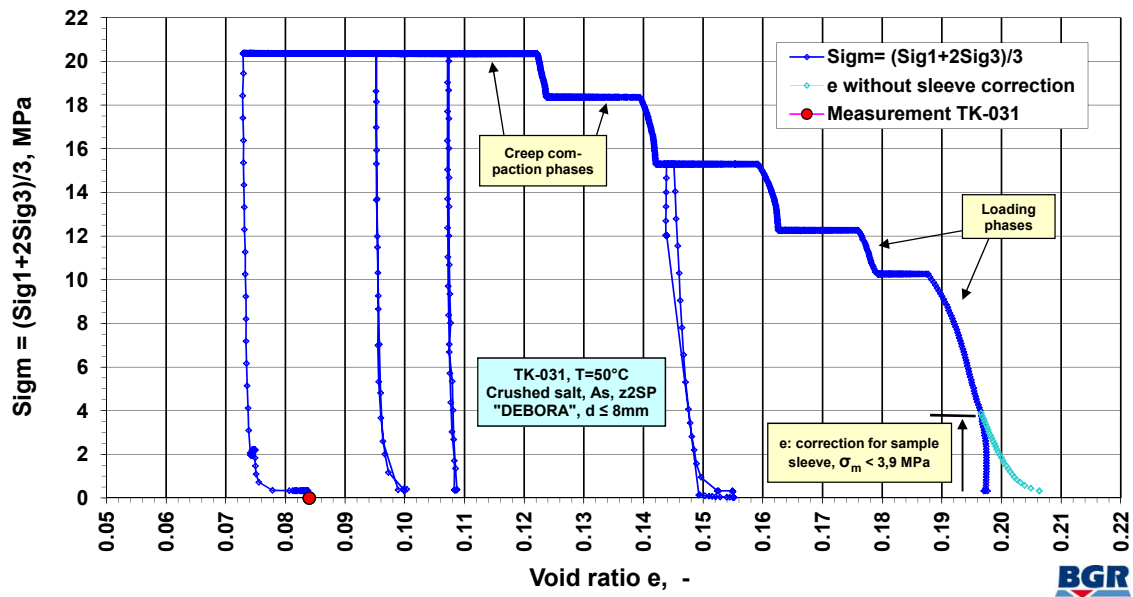
R & D Radioactive Waste Repository
STÜHRENBERG, D.(2013): Triaxial Compaction Test TK-031
Evaluation Report; Hannover (BGR)

Page 13 of 33

Fig. 5:   Stress-void ratio diagram for test TK-031

3.4   Measurement of the compacted test specimen

When removed from the apparatus, the test specimen showed the expected hourglass shape (Fig.6). To preserve the specimen for further investigations, it was not cut into several slices and faced, as was undertaken in preceding tests for the purposes of precisely determining the density, instead, it was measured several times using a calliper gauge. The volume can be determined with the necessary degree of accuracy by measuring the diameter in steps of 1 cm down the specimen and three times at each position (120° rotation) alongside the measurement of the height at three positions.

The calliper gauge measurement after removing the specimen from the apparatus revealed a specimen height of h = 191.14 mm. It has therefore been compacted by 5.4 mm compared to its original state. The diameters determined for each virtual slice, and which varied between (99.0 > d > 95.6 mm) were combined with the height to give a specimen volume of V_E = 1399 cm^3. The sample has therefore been compacted by around 144 cm^3 as a result of being exposed to the triaxial load, and was therefore calculated to only contain a pore space of approx. 110 cm^3. The mean diameter derived from several measurements has therefore decreased by approx. 3.5 mm to 96.5 mm. (Error assessment: if the diameter was measured around 0.2 mm too wide because of the roughness of the outer surface of the specimen, this would correspond to an additional volume of approx. 6 cm^3 or Δe = 0.0045). The sample was weighed and this revealed a mass of m = 2800.4 g. This was around 3.7 g more than measured when the pre-compacted specimen was installed

R & D Radioactive Waste Repository
STÜHRENBERG, D.(2013): Triaxial Compaction Test TK-031
Evaluation Report; Hannover (BGR)

Page 14 of 33

in the triaxial cell, but is almost exactly the same amount measured when the crushed salt mass was filled into the cylinder prior to pre-compaction. This difference is unusual and defies explanation.
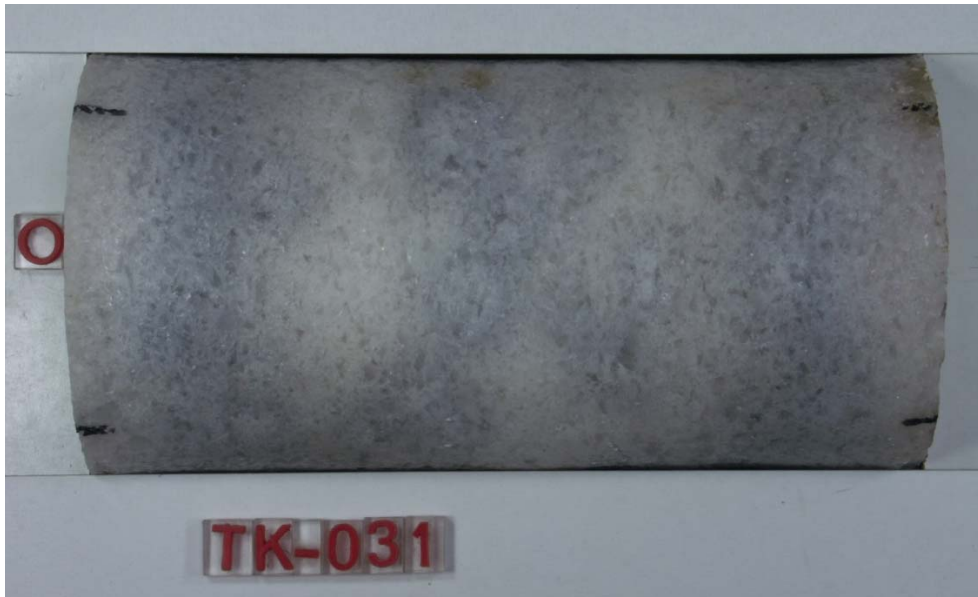

Fig. 6:   Test specimen TK-031 after the test

It is not possible to exclude the existence of a measurement error when installing the specimen ready for the triaxial test. It is also possible that the evaporated fluid level oil was partially absorbed by the specimen and thus had an effect on the weight of the specimen. However, the difference between the various values is only $\Delta e = 0.001$. The "final value" for the density and the void ratio are therefore:

$\rho^f_E = 2.002$ g/cm³ und $e_E = 0.084$

3.5   Calculation of the compaction volume

In the following "final evaluation", the values determined from the completely depressurised sample were used as the target parameters. The volumetric expansion curve determined in the test-related calculation was scaled accordingly. Nevertheless, the pressure release and temperature lowering phases of the test are associated with uncertainties because the (elastic re-)strain in the specimen as a result could not be recorded by the pore volume measurement. The measured values are superimposed by the behaviour of the specimen sleeve in particular as the confining pressure increasingly declines. The differential value of $\Delta e = 0.01$ interpreted in the calculation as deconsolidation, and which corresponds to the

R & D Radioactive Waste Repository
STÜHRENBERG, D.(2013): Triaxial Compaction Test TK-031
Evaluation Report; Hannover (BGR)

Page 15 of 33

amount of compaction progression in the last 60 days of the test, is therefore uncertain. However, the overall influence on the creep rates determined in the following remains minor.

The following facts, assumptions and corrections are added here to supplement Chapter 3.3 and 3.4:

1. Axial length change/sample height: an elongation of the sample of 0.07 mm was measured during the warming up phase under the technical pre-load of approx. 6 kN axial and 1 bar radial. It was reset to 0 at the beginning of the first loading phase. No axial contribution to the measured value attributable to the deformation of the O-ring was observed (see Chapter 3.2). The shrinkage of the sample registered at the end of the test during the cooling down phase from 50 to 30 °C was 0.09 mm.

2. Volume measurement/calculation: the compaction is calculated beginning with the first load phase at t = 3.8 days. Changes in the shape of the specimen during the warming up phase were ignored.

During the initial phases of the 1st loading phase (3.82 < t < approx. 5.0 days) an overproportional loss in volume was observed as seen in previous tests. This is assumed to be an artefact of the sleeve surrounding the specimen and should therefore not be interpreted as reflecting true compaction of the sample. The values measured during this time period are adjusted lower as shown in Fig. 5 at the beginning of the loading at the e = 0.2 range. The compaction measured in an axial direction serves as the qualitative reference value for this purpose. The deducted volume (V_v) from t = 5.0 d totals 12.0 cm^3 ($\Delta e \approx 0.009$).

The test-associated evaluation of the compaction is calculated as too high when using the C_3 values derived from the calibration tests AVOL-B110 and AVOL-B111 (Fig. 2), when these are compared with the target value derived from the measurement after removing the specimen from the apparatus (e = 0.067 instead of 0.084; Δ = 0.017). To compensate for this difference, the new C_3 factors used after each "venting" are lowered. The values dependent on the void ratio and the system volume shown in the plots are approximately linear and were therefore shifted parallel ($\Delta C_3 \approx 0.33$), to give the red line visualised in Fig. 2 with the reference points required in test TK-031.

The density and void ratio are then evaluated using the value m = 2797.7 g. In accordance with Chapter 2.2, Fig. 7 shows the crucial measurement, calculation and correction curves as a function of time needed to determine the compaction volume occurring in the test. The magenta-coloured curve "VB1" with respect to the primary axis, shows the registered fluid levels of measurement burette B20 used in this instance. The B20 level was reset a total of eight times by "venting" because of the limited capacity of the burette. Aggregation

R & D Radioactive Waste Repository
STÜHRENBERG, D.(2013): Triaxial Compaction Test TK-031
Evaluation Report; Hannover (BGR)

Page 16 of 33

of the VB1 values taking into consideration a measurement error associated with the loss of fluid level liquid gives rise to the green plot "total-Vf+K1". The proportion associated with the loss in fluid was determined in separate calibration tests and is shown as a bright red plot "corr. liquid level oil loss (K1)" in Fig. 7 with respect to the secondary axis. Please note the difference in the scaling of the primary and the secondary axis (factor 2).
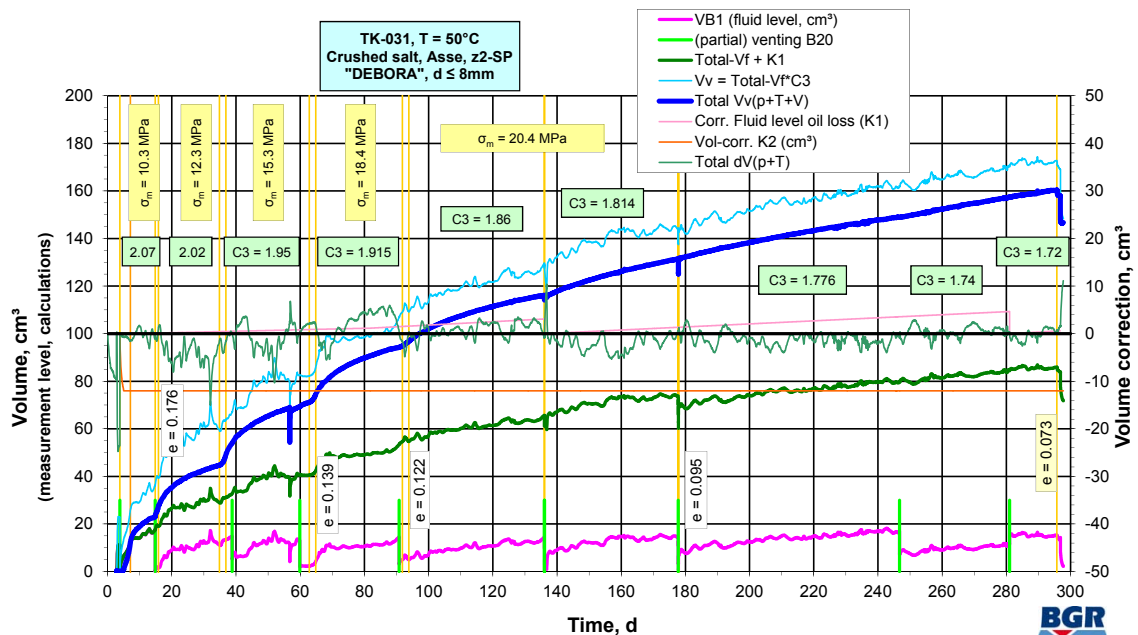

Fig. 7:   Measurement, calculation and correction plots for TK-031

To determine the volume of air in an uncompressed state squeezed out of the specimen, the fluid level values were multiplied by the specified C_3 factors in each of the phases. The resulting curve V_v (light blue) oscillates primarily because of the continuous fluctuations in atmospheric pressure. The volume compaction in cm^3 units is derived by superimposing the correction values from the air pressure and temperature fluctuations (total dV(p+T)) and the correction values from the sample sleeve "Vol-corr. K2" (see above). The blue plot "GVv (p+T+V)" shows the result.

3.6   Detailed test procedure and results

The following chapter describes in detail the course of the test with the subsequent evaluation and the results this produced. Significant milestones during the test are documented quantitatively in Table 1.

R & D Radioactive Waste Repository
STÜHRENBERG, D.(2013): Triaxial Compaction Test TK-031
Evaluation Report; Hannover (BGR)

Page 17 of 33

Tab. 1: Chronology of test TK-031

TK-031 (As-z2HS-Sp), T = 50 °C, w ≈ 0,05 wt-% - 14.11.2011 - 07.09.2012 — C3 (7)

#	Event	C3 adjustment (7)	Date	Test time t, d	F_1, kN	Sig1, MPa	Sig3, MPa	Sample volume V, cm³	Sample hight H, mm	Calc. Cross-section A, cm²	Eps1= dH/Ho, %	Ev= PrV√V0, %	Void ratio e, RhoSf= 2,170 g/cm³	Porosity Φ, %
	$V_0, h_0, A_0, e_0, \Phi_0 =$							1543.5	196.53	78.54			0.1973	16.48
1	From 9:10: setting up pre-load, 14:00: start recording data without measuring the volume		14.11.2011 14:00	0.000	-6.0	0.77	0.10	1543.5	196.53	78.54	0.00	0.00	0.1973	16.48
2	Volume measurement calibrated	2.070	17.11.2011 07:47	2.741	-6.1	0.77	0.10	1543.5	196.53	78.54	0.00	0.00	0.1973	16.48
3	Cell heating system switched on, warming up time approx. 8 h		17.11.2011 10:00	2.833	-6.1	0.77	0.10	1543.1	196.53	78.52	0.00	0.00	0.1969	16.45
4	(1st) venting B20 (9:45)	2.070	18.11.2011 09:45	3.823	-6.0	0.77	0.10	1544.0	196.53	78.56	0.00	0.00	0.1976	16.50
5	Start 1st loading (3.0 MPa/d)		18.11.2011 10:00	3.833	-6.1	0.77	0.10	1543.6	196.53	78.54	0.00	0.00	0.1973	16.48
6	Stop F1/Sig3: End loading phase 1		21.11.2011 16:00	7.083	-84.6	10.78	10.00	1531.2	196.25	78.02	0.14	0.80	0.1877	15.81
7	1st compaktion phase: Sigm = 10.26 MPa				-84.6	10.78	10.00				0.00	0.00		
8	(2nd) venting B20 (9:00, 9:52)	2.020	29.11.2011 09:02	14.793	-84.6	10.79	10.00	1520.5	196.00	77.58	0.27	1.49	0.1794	15.21
9	Start 2nd loading (2.0 MPa/d)		29.11.2011 10:00	14.833	-84.6	10.79	10.00	1520.4	196.00	77.57	0.27	1.50	0.1793	15.21
10	Stop F1/Sig3: end loading phase 2		30.11.2011 10:00	15.833	-100.3	12.79	12.00	1516.1	195.91	77.39	0.31	1.78	0.1760	14.97
11	2nd compaktion phase: Sigm = 12.26 MPa				-100.3	12.79	12.00				0.00	0.00		
12	Start 3. loading (1.5 MPa/d)		19.12.2011 10:00	34.833	-100.3	12.79	12.00	1500.1	195.42	76.77	0.57	2.81	0.1636	14.06
13	Stop F1/Sig3: end loading phase 3		21.12.2011 10:00	36.833	-124.5	15.88	15.00	1494.5	195.20	76.56	0.68	3.18	0.1592	13.74
14	3rd compaktion phase: Sigm = 15.29 MPa				-124.5	15.88	15.00				0.00	0.00		
15	(3rd) partial venting B20 (9:26)	1.950	23.12.2011 09:27	38.810	-124.5	15.88	15.00	1489.5	195.01	76.38	0.77	3.50	0.1554	13.45
16	Start unloading because of power shut-down		10.01.2012 07:22	56.724	-124.5	15.89	15.00	1474.7	194.41	75.85	1.08	4.46	0.1439	12.58
17	B20 shut off: 7:46 - 8:03		10.01.2012 07:46	56.740	6.0	0.01	0.05	1488.3	194.55	76.50	1.01	3.58	0.1544	13.38
18	Loading "positive connection" (7:58)		10.01.2012 07:58	56.749	-6.0	0.78	0.04	1489.0	194.55	76.53	1.01	3.53	0.1550	13.42
19	Reloading completed		10.01.2012 10:10	56.840	-124.5	15.88	14.99	1476.3	194.41	75.93	1.08	4.36	0.1451	12.67
20	Contin. 3rd Comp. phase: Sigm = 15.29 MPa				-124.5	15.88	15.00				0.00	0.00		
21	(4th) partial venting B20 (10:41, 10:44)	1.915	13.01.2012 10:42	59.862	-124.5	15.89	15.00	1474.2	194.34	75.85	1.11	4.49	0.1435	12.55
22	Start 4th loading (1.5 MPa/d)		16.01.2012 10:00	62.833	-124.5	15.89	15.00	1472.4	194.29	75.79	1.14	4.61	0.1421	12.44
23	Stop F1/Sig3: End loading phase 4		18.01.2012 10:00	64.833	-149.5	19.08	17.99	1469.0	194.11	75.68	1.23	4.83	0.1394	12.24
24	4th compaction phase: Sigm = 18.36 MPa				-149.5	19.08	18.00				0.00	0.00		
25	(5th) partial venting B20 (9:02)	1.86	13.02.2012 10:03	90.835	-149.5	19.09	18.00	1449.2	193.10	75.05	1.75	6.11	0.1241	11.04
26	Start 5th loading (1.0 MPa/d)		14.02.2012 10:00	91.833	-149.5	19.09	17.99	1448.7	193.08	75.03	1.76	6.14	0.1237	11.01
27	Stop F1/Sig3: End loading phase 5		16.02.2012 09:50	93.826	-165.1	21.07	19.99	1446.8	192.98	74.97	1.80	6.27	0.1222	10.89
28	5th compaction phase: Sigm = 20.35 MPa				-165.1	21.07	19.99				0.00	0.00		
29	Unloading (15 min): F1 to 8 kN, Sig3 to 0		29.03.2012 15:42	136.071	-165.1	21.09	19.99	1427.4	191.99	74.35	2.31	7.53	0.1072	9.68
30	(6th) venting B20 because of unloading (15:50)	1.814	29.03.2012 15:52	136.078	-60.6	7.77	6.68	1427.7	192.07	74.34	2.27	7.50	0.1075	9.70
31	Approx. 6 cm³ fluid level oil topped up		29.03.2012 16:05	136.087	-7.9	1.07	0.00	1429.1	192.13	74.38	2.24	7.42	0.1085	9.79
32	Reloading completed		29.03.2012 16:28	136.103	-165.1	21.08	19.99	1427.7	192.00	74.36	2.30	7.50	0.1074	9.70
33	Heating regulator failure: temperature reduction in the cell		29.03.2012 16:50	136.118	-165.1	21.08	19.99	1427.8	192.00	74.36	2.30	7.50	0.1075	9.71
34	Tz=34.8 °C, regulator repaired (8:38)		30.03.2012 08:38	136.777	-165.1	21.08	19.99	1427.3	191.90	74.38	2.35	7.53	0.1071	9.68
35	Tz=50,4°C: T constant again		31.03.2012 06:00	137.667	-165.1	21.08	19.99	1427.2	191.96	74.35	2.32	7.54	0.1070	9.67
36	Continuation 5th compaction phase: Sigm = 20.35 MPa				-165.1	21.09	20.00				0.00	0.00		
37	Unloading (45 min): F1: 5 kN, Sig3: 0		10.05.2012 08:00	177.750	-165.1	21.09	20.00	1412.0	191.43	73.76	2.59	8.52	0.0953	8.70
38	(7th) venting B20 because of unloading (8:20, 9:59)	1.776	10.05.2012 08:30	177.771	-58.5	7.50	6.81	1412.7	191.51	73.76	2.55	8.48	0.0958	8.74
39	Start of reloading (2 h)		10.05.2012 10:00	177.833	-6.0	0.80	0.20	1418.0	191.61	74.00	2.51	8.14	0.0999	9.08
40	Reloading completed		10.05.2012 12:00	177.917	-164.6	21.03	19.93	1412.0	191.44	73.75	2.59	8.52	0.0952	8.69
41	Cont. of 5th comp. phase: Sigm = 20.35 MPa				-165.1	21.10	19.99				0.00	0.00		
42	Air conditioning defective (room temp., 3.5 d)		27.06.2012 16:00	226.083	-165.1	21.10	19.99	1398.8	191.09	73.20	2.77	9.38	0.0850	7.83
43	(8th) partial venting B20 (6:51)	1.740	18.07.2012 06:52	246.703	-165.1	21.10	19.99	1394.6	190.97	73.02	2.83	9.65	0.0817	7.56
44	Air conditioning defective (room temp., 3 d)		19.08.2012 12:00	278.917	-165.1	21.11	20.00	1386.6	190.83	72.66	2.90	10.17	0.0756	7.03
45	6 cm³ fluid level oil topped up	1.720	21.08.2012 13:38	280.985	-165.1	21.11	20.00	1386.2	190.82	72.65	2.91	10.19	0.0752	7.00
46	Air conditioning defective (room temp., 2 d)		25.08.2012 00:00	284.667	-165.1	21.11	19.99	1385.2	190.81	72.60	2.91	10.26	0.0745	6.93
47	Start unloading (6.3 MPa/d, to 15 kN / 2 MPa)		05.09.2012 08:00	295.750	-165.1	21.11	19.99	1383.2	190.76	72.51	2.94	10.39	0.0729	6.79
48	Pre-load reched		05.09.2012 11:02	295.876	-14.9	1.89	2.00	1384.9	190.88	72.55	2.87	10.28	0.0742	6.91
49	Raise F1 (4 min) to 20 kN		05.09.2012 15:16	296.053	-15.9	2.03	2.00	1385.3	190.90	72.57	2.87	10.25	0.0745	6.94
50	2 cm³ fluid level oil topped up		06.09.2012 07:16	296.719	-20.0	2.59	2.00	1385.7	190.89	72.59	2.87	10.23	0.0748	6.96
51	Start of unloading (6 min) to 6 kN / 0.1 MPa)		06.09.2012 10:10	296.840	-20.0	2.59	2.00	1385.9	190.89	72.60	2.87	10.22	0.0750	6.97
52	Heating switched off (T = 50°C)		06.09.2012 10:23	296.849	-6.0	0.82	0.10	1395.0	190.91	73.07	2.86	9.63	0.0820	7.58
53	End of automatic test log (T≈32°C)		07.09.2012 08:00	297.750	-6.0	0.82	0.10	1396.8	190.82	73.20	2.91	9.50	0.0835	7.71
	Removal of the specimen: 07.09.12													
	Measurement of the specimen: 12.09.13 / 14.09.13							1399	191.0				0.0840	7.76

R & D Radioactive Waste Repository
STÜHRENBERG, D.(2013): Triaxial Compaction Test TK-031
Evaluation Report; Hannover (BGR)

Page 18 of 33

If the volumetric compaction curve GVv pursuant to equation (7) shown in Fig. 7 is compared to the initial value of 1543.6 cm³, this gives the volumetric strain ε_v already shown in Fig. 7 as a dimensionless parameter. The derivative against time is the volumetric strain rate $\dot{\varepsilon}_v$, calculated using the reduced data volume. These test results are shown in Fig. 8 and Fig. 9 for the first 4 loading phases where σ_3 = 10, 12, 15 and 18 MPa (0 d < t < 100 d) or for the 5th load phase with σ_3 = 20 MPa (80d < t < 300 d) blue (ε_v) and red ($\dot{\varepsilon}_v$).
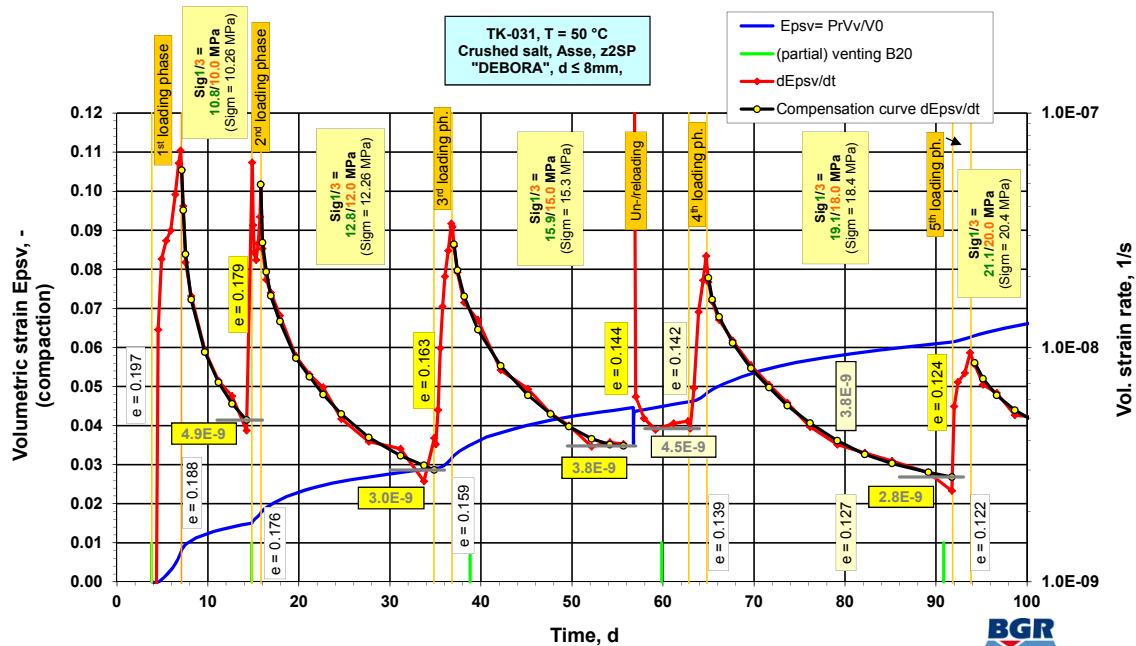
Fig. 8:   TK-031- Volume strain, volume strain rate and compensation curves, part 1
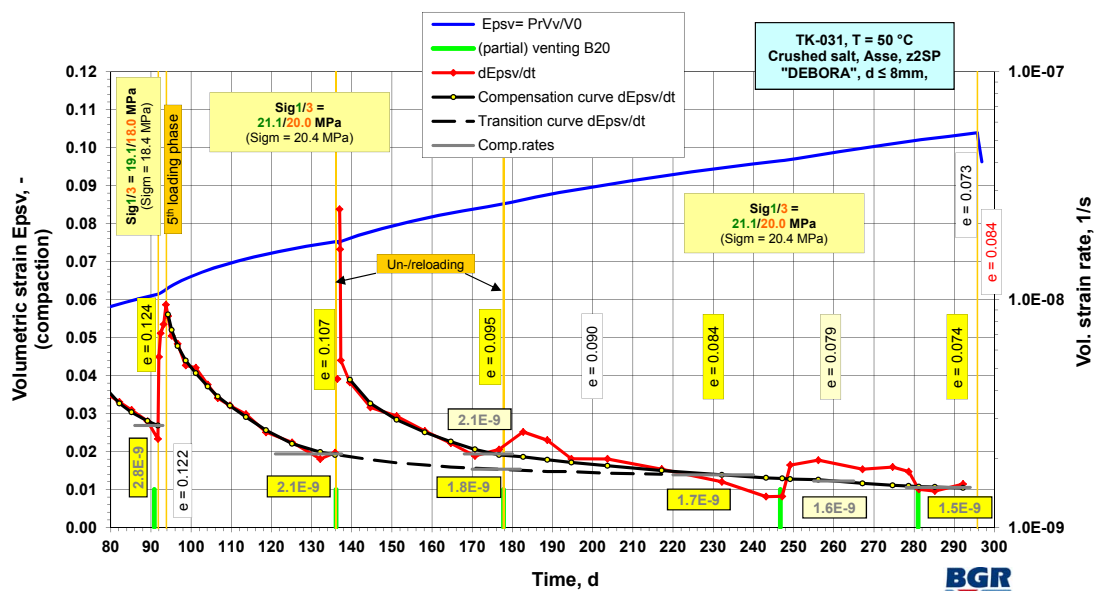
Fig. 9:   TK-031- Volume strain, volume strain rate and compensation curves, part 2

R & D Radioactive Waste Repository
STÜHRENBERG, D.(2013): Triaxial Compaction Test TK-031
Evaluation Report; Hannover (BGR)

Page 19 of 33

To be able to reliably interpret the still remaining oscillations or the fluctuations in the curves caused by the interruptions to the test, and the way the aforementioned affect the compaction rates, the trend curves have been manually adjusted in the results (black). The jump in the curve after the 2nd power outage (t = 136 d, see below) was also manually compensated for. The compaction rates and the associated void ratios determined from the results of the tests are shown in the figures at the representative positions in the test.

The sample was heated up to 50 °C after 3 days under a pre-load of F_1 = 6 kN and σ_3 = 0.77 MPa (line no. 3 in Tab. 1). The constant temperature was reached after approx. 8 hours. The fluid level in burette B20 rose to 11 cm^3 because of thermal expansion in the measurement system. The system was therefore "vented" before the beginning of the 1st loading phase. The quasi-hydrostatic load of the 1st (creep)-compaction phase of σ_1 = 10.8 and σ_3 = 10.0 MPa was reached at approx. 3 MPa/d within 3 days and 6 hours. The stress-dependent loading rates were deliberately kept low in test TK-031 so that the resulting rise in the compaction rates was not higher than around $1.0 \cdot 10^{-7}$ s^{-1}.

The compaction rates $\dot{\varepsilon}_v$ < $1.0 \cdot 10^{-8}$ s^{-1} recorded in phase 1 immediately after the start of loading (t = 3.83 d) are calculated from the implemented volume correction (sample sleeve) and should therefore not be interpreted as material-specific behaviour.

The 1st creep compaction phase (σ_m = 10.26 MPa) was ended after 7 days because of the aspects explained in Chapter 3.7. The volumetric compaction rate had dropped below $5 \cdot 10^{-9}$ s^{-1} with a degressive trend. The void ratio was e = 0.179. The value for this compaction state is defined as $4.9 \cdot 10^{-9}$ s^{-1} with the compensation curve.

After "venting" the measuring apparatus, the 2nd compaction phase was reached with σ_1 = 12.8 and σ_3 = 12.0 MPa (σ_m = 12.26 MPa) under a loading rate of approx. 2 MPa/d. This phase lasted 19 days and ended at e = 0.163, where $\dot{\varepsilon}_v$ = $3 \cdot 10^{-9}$ s^{-1}.

The quasi-hydrostatic load with 1.5 MPa/d was raised to σ_1 = 15.9 and σ_3 = 15.0 MPa for the 3rd compaction phase (σ_m = 15.29 MPa, line no. 13 in Tab. 1) (34.8 < t < 36.8 d). The volume measurement apparatus was partially vented on d = 38. After approx. 20 days (56th test day), the volumetric compaction rate had declined to approx. $3.8 \cdot 10^{-9}$ s^{-1} (e = 0.144).

The sample then had to be temporarily depressurised for the first time because of a power outage. The burette fluid level dropped considerably during the depressurisation because of the elastic strain of the sample and the assumed re-strain of the sample sleeve. The feed pipe was shut off when it reached 4 cm^3 to prevent any fluid level oil from penetrating the piping system. After re-establishing the load, it was initially not possible to reach the previous measured value (ΔV_{oil} = -1.3 cm^3), whereby the calculated void ratio rose by 0.001.

The total duration of the depressurisation and loading process was 2 hours and 48 minutes. After a 2-day transition phase, the volumetric compaction rate of $\dot{\varepsilon}_v = 4.5 \cdot 10^{-9}$ s^{-1} at e = 0.142 was almost constantly higher than prior to the intervention ($\dot{\varepsilon}_v = 3.8 \cdot 10^{-9}$ s^{-1}, e = 0.144).

The 4th partial venting took place on d = 59. On the 62nd test day, the load was again raised by 1.5 MPa/d to σ_1 = 19.1 and σ_3 = 18.0 MPa (σ_m = 18.4 MPa) for the 4th loading phase. After 27 days under this load, $\dot{\varepsilon}_v = 2.8 \cdot 10^{-9}$ s^{-1} at e = 0.124 were measured or calculated respectively. The 5th partial venting was undertaken one day prior to the next increase in load (t = 90.8 d).

After the 2-day 5th loading phase, the associated creep compaction phase began on the 93rd test day at e = 0.122 where σ_1/σ_3 = 21.1/20.0 MPa (σ_m = 20.4 MPa).

The planned final loading phase of σ_1/σ_3 = 21.1/20.0 MPa (σ_m = 18.4 MPa) at a rate of 1.0 MPa/d was applied on the 92nd and 93rd test day. This loading phase was run for a total of 102 days from a void ratio of e = 0.122, but had to be interrupted on the 136th and 177th test days for a few hours because the power had to be turned off.

The depressurisation No. 2 of test TK-031 on the 136th day (Fig. 9) only lasted 46 minutes. However, the heating failed for several hours as a consequence, and this caused the cell temperature to drop from 50 to 35 °C. The set value only stabilised at a constant level again after 1.5 days. During this depressurisation, the volume measurement apparatus was also vented. This revealed that 6 cm3 of fluid level oil had already evaporated out of the open system because of the long duration of the test. The lost amount was topped up and the effects on the measurements were taken into consideration accordingly in the final evaluation.

Because of these influences, and reestablishment of the loading at σ_m = 20.4 MPa, the determined compaction rates revealed a much longer transition phase than determined during the previous interruption on the 56th day, and the 3rd depressurisation and reloading which occurred on the 177th day. Up until then, the compaction rate $\dot{\varepsilon}_v$ only dropped to a range of 2.1$\cdot$10^{-9} s^{-1} (e = 0.095). The intervention on the 177th day with the venting of the measurement apparatus lasted 4 hours. The subsequent transition phase with a slightly raised compaction rate was considered to have come to an end after 15 days. This is when sample compaction continued again under a slightly lower compaction rate.

With the exception of occasional fluctuations in room temperature, test TK-031 continued to run according to plan. The measurement apparatus was partially vented on the 24th and 280th test day (No. 7 and 8). The system was topped up again with 6 cm^3 fluid level oil during the 8th partial venting. A notable aspect is that despite the unchanged load between

R & D Radioactive Waste Repository
Stührenberg, D.(2013): Triaxial Compaction Test TK-031
Evaluation Report; Hannover (BGR)

Page 21 of 33

these two partial venting episodes, the calculated compaction rate was constantly at a slightly higher level ($1.8 \cdot 10^{-9}$ s^{-1} - $2.1 \cdot 10^{-9}$ s^{-1}).

On the 295th day, the sample was depressurised from σ_1/σ_3 = 21.1/20.0 MPa to 2.5/2.0 MPa. The axial re-strain (sample elongation) was 0.13 mm and the displaced pore air volume decreased by 2.0 cm^3. During the following 19 hours, the measured pore air volume declined by another 0.7 cm^3 even though the length of the specimen remained virtually unchanged. The calculated void ratio rose from e = 0.073 to 0.075 because of the re-strain.

The following depressurisation down to σ_1/σ_3 = 0.8/0.1 MPa caused the sample to lengthen by another 0.02 mm, and the registered backflow of air into the sample was almost 10 cm^3 with a still rising trend. After switching off the heating, the test was terminated after a total duration of 297 days.

3.7 Evaluation of the results of TK-031

The main objective of the test is to determine the compaction rates expected in the residual porosity range under the relevant site-specific conditions, i.e. under external stresses of not more than around 20 MPa. To achieve this under test conditions, however, the specifications for the loading phases have to exceed the generally expected in situ convergence rates as a reaction of the sample.

The results shown in Figs. 8 and 9 show the typical course of the compaction rates for the selected loading paths: after a strong rise in the phases with rising loads (load increases), there is a degressive decline in the curve as soon as the load is maintained at a constant level.

In the 5 loading phases where $3.0 \geq \dot{\sigma} \geq 1.0$ MPa/d the evaluation undertaken here reveals that maximum compaction rates of between $\dot{\varepsilon}_v$ = $6.9 \cdot 10^{-8}$ s^{-1} and $9.5 \cdot 10^{-9}$ s^{-1} are reached. The peak values decline successively with decreasing void ratios despite an increase in the load, which is attributable to the deliberately selected step-wise decrease in the loading rates $\dot{\sigma}$. The higher compaction rates are therefore overall in a range which is not expected to have any significant impact on the material properties. The material behaviour registered in the subsequent creep compaction phases can therefore be considered representative in this respect for the relevant in situ conditions after an appropriate transition phase. Table 2 shows an overview of the compaction rates reached at the end of the loading phases (load increases) in this evaluation.

R & D Radioactive Waste Repository
STÜHRENBERG, D.(2013): Triaxial Compaction Test TK-031
Evaluation Report; Hannover (BGR)

Page 22 of 33

Tab. 2:   Volumetric compaction rates at the end of the load increases

σ_m	Triaxial compaction test TK-031, T = 50 °C Compaction rates at the end of the load increases			
	t, d	**e, -**	ε_v **, %**	$\dot{\varepsilon}_v$ **, s^{-1}**
10.3	7.1	0.188	0.75	$6.9 \cdot 10^{-8}$
12.3	15.8	0.176	1.77	$5.0 \cdot 10^{-8}$
15.3	36.8	0.159	3.15	$3.4 \cdot 10^{-8}$
18.4	64.8	0.140	4.81	$2.5 \cdot 10^{-8}$
20.4	93.7	0.122	6.26	$9.5 \cdot 10^{-9}$

Because of the continuing increase in the density of the sample, it is not possible for the compaction rate to achieve a constant value under unchanging load. The compaction rate which develops under a defined load, and in the presence of a specific void ratio, can be determined from the test when the influence of the step-wise loading increases has fallen off. An indication of this in this type of test is when the oscillation of the compaction rate increases considerably even when taking into consideration larger time intervals, i.e. of the order of 3-5 days. The amount of time required for the test to produce reliable results increases with the decreasing porosity of the material. The points in time for the increases in load were selected in accordance with these aspects during the ongoing evaluation of the test. The value reached at the end of the creep compaction phases is then evaluated as the result for the compaction phase reached in each case, as was done in the previous tests (STÜHRENBERG, 2002).

It is important to realise that there is a not inconsiderable sensitivity to interruptions to the test in the residual porosity range under lower compaction rates. The associated effects can only be compensated for by investing a considerable amount of time. In the case of the first interruption on the 56th test day (cf. Chapter 3.6), the volumetric strain rate of $\dot{\varepsilon}_v = 4.5 \cdot 10^{-9}$ s^{-1} determined after the reloading phase and up until the load increase undertaken on t = 62.8 d, was calculated as around 18 % higher than the volumetric strain rate prior to the test interruption. It is assumed that the results would have followed a qualitatively similar trend if the load had remained unchanged beyond the time t = 62.8 d, as in the 5th creep compaction phase, which was also affected by problems. However, an additional test duration of several weeks would be required to make the necessary verification of the presence of converging compaction rates.

Phase 5 which was planned to look at long-term creep compaction, was negatively affected by 2 unforeseen depressurisation steps caused by problems with test operations. In this instance, the significantly raised volumetric strain rate which appeared after the interruption at t = 136.1 d only declined in this time-dependent visualisation after a period of 70 – 80 days to the trend which would have been expected if the interruption had not taken place. The dashed line from t = 136.1 d shown in Fig. 9 is used as the plausible transition curve. The targeted measurement accuracy is highlighted by the red value curve in the subsequent course of the test.

The values highlighted in yellow and entered for various points in time in Figs. 8 and 9 are used for the comparison with the results in STÜHRENBERG (2002), Chapter 4.3. They are valid for the compaction and loading state calculated in each case (void ratio, stress) of test TK-031, and are summarised numerically in Tab. 3.

Tab. 3:   TK-031: Volumetric compaction rates, creep compaction phases

σ_m, MPa	Triaxial compaction test TK-031, T = 50 °C Compaction rates at the end of the creep compaction phases			
	t, d	e, -	ε_v , %	$\dot{\varepsilon}_v$, s^{-1}
10.3	14	0.179	1.48	$4.9 \cdot 10^{-9}$
12.3	34	0.163	2.89	$3.0 \cdot 10^{-9}$
15.3	55	0.144	4.41	$3.8 \cdot 10^{-9}$
18.4	91	0.124	6.11	$2.8 \cdot 10^{-9}$
20.4	135	0.107	7.51	$2.1 \cdot 10^{-9}$
	177	0.095	8.50	$1.8 \cdot 10^{-9}$
	230	0.084	9.44	$1.7 \cdot 10^{-9}$
	290	0.074	9.87	$1.5 \cdot 10^{-9}$

Volumetric compaction rates of $4.9 \cdot 10^{-9}$ s^{-1} > $\dot{\varepsilon}_v$ > $1.5 \cdot 10^{-9}$ s^{-1} were determined in the investigated void ratio range of 0.179 > e > 0.074. The range of the compaction rates with only around half an order of magnitude is remarkably small despite the significant differences in stress (Δσ = 10 MPa).

R & D Radioactive Waste Repository
STÜHRENBERG, D.(2013): Triaxial Compaction Test TK-031
Evaluation Report; Hannover (BGR)

Page 24 of 33

3.8 Comparison with odometer test results

The results of several triaxial compaction tests were compared with those from displacement controlled odometer tests in a stress-void ratio diagram in STÜHRENBERG (2002), Chapter 4, with the aim of quantitatively correlating the odometer test results in three-dimensional stress space, and initially also to limit the scatter in the results arising from the triaxial tests.

The result parameter "backfill resistance" ("σ_1") determined from the odometer tests cannot be used directly as a comparative parameter because of the inhomogeneous stress state. The mean stress σ_m pursuant to equation (4) is therefore estimated with a stress ratio defined by KORTHAUS in BECHTHOLD et al. (1999):

$$\beta(\Phi) = \sigma_3/\sigma_1 = 0,105 - 0,193 \ln(\Phi) \tag{17}$$

The relationship was derived from tests on cube-shaped crushed salt samples carried out in an autoclave. Even though their validity for low porosities has not been verified, the isolines for constant compaction rates from the odometer tests generated in this way were also used here for trend orientation purposes.

As reported in STÜHRENBERG (2002), the Oedo-049 test undertaken in 1994 with crushed salt from the Asse mine (z2HS), where T = 50 °C, d_{max} = 31.5 mm (drift backfill), is used for the comparison test. Because of the more stringent demands for accuracy, the results of the Oedo-049 test were re-evaluated. Instead of the rock salt density of 2.16 g/cm³ and moisture content of 0.5 % assumed at the time, the re-evaluation uses a solid material density of ρ_S^{tr} = 2.1784 g/m³ calculated in KRÖHN (2009), Chapter 4.4.2 for Asse crushed salt z2HS, and a moisture content of 0.1 %, which is considered to be a more realistic assessment of the in situ moisture. The reference value for the void ratio of the material including its moisture content is therefore ρ_S^{tr} = 2.1806 g/m³. However, the difference between this and the previous evaluation is only minor. In the case of the backfill resistance curves, the void ratios are now higher and between 0.0055 and 0.0050. The influence of the existing material difference (TK-031: Asse, z2SP "Table salt") and the sieve curve for borehole backfill where d_{max} = 8 mm, KRÖHN (2009), Chapter 4.10, is also considered to be fairly minor. In a similar way to the comparison of the material forming the Hauptsalz in the Asse mine and in Gorleben (STÜHRENBERG, 2002), the differences (scatter) overall can be assumed to be in the range of one order of magnitude with respect to the compaction rates in the σ_1-e-diagram.

Fig. 10 shows the results of the Oedo-099 test with the 4 different compaction speeds separated by one order of magnitude (isolines) and creep compaction rates of test TK-031 (violet) given in Tab. 3. To highlight the whole range, the compaction rates shown in Table 2 and determined at the end of the load increase phase are also shown (pink). Because of the higher void ratio, they are always shown to the right in the relevant load phase in Fig. 10.
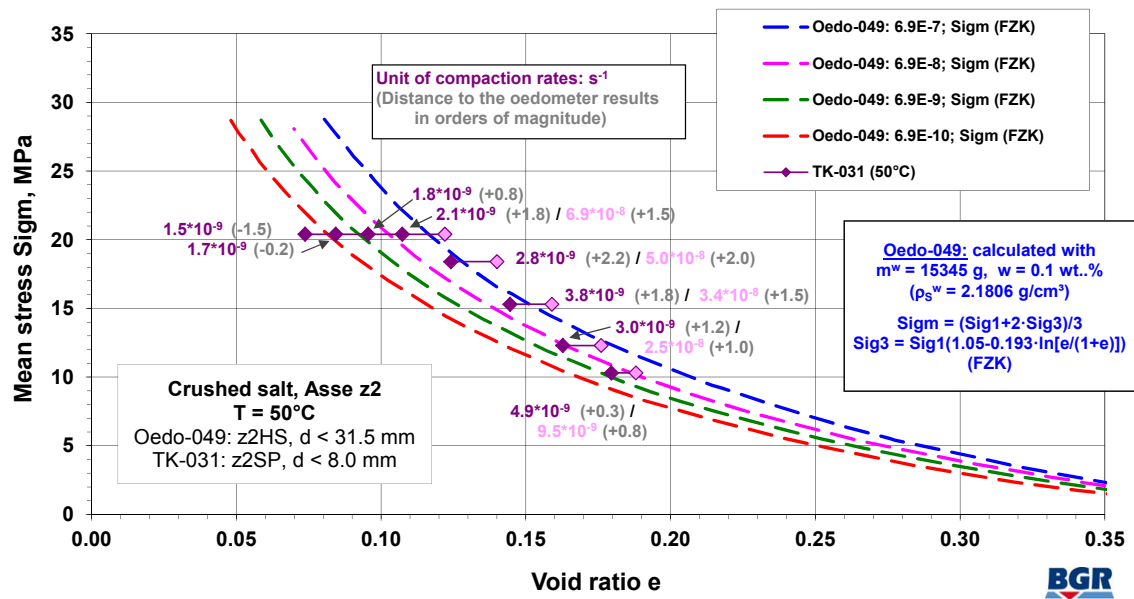
Fig. 10: Comparison of the results of TK-031 with the odometer data (FZK-estimated value)

The order of magnitude of the separation between the isolines of the same odometer results are selected as the scale for the comparison. They are shown in Fig. 10 as the grey numbers in brackets behind the compaction rates. The values with the same rates which lie closer to the origin in the diagrams indicate more favourable material behaviour in the sense of the fastest possible compaction as a result of the convergence of the rock mass (shown as negative values in Fig. 10).

The compaction rates at the end of the first four phases with constant loads σ_m = 10.3 to 18.4 MPa ($\dot{\varepsilon}_v$ = $4.9 \cdot 10^{-9}$ to $2.8 \cdot 10^{-9}$ s^{-1}, Tab. 3) are around 0.3 to 2.2 orders of magnitude higher than the comparative values from the Oedo-049 test. The same already applied to the compaction rates according to Tab. 2 at the beginning of each load phase. This rising trend does not continue for the first defined value of the 20.4 MPa phase. The compaction rate lies only around 1.8 to 1.5 orders of magnitude higher than the corresponding odometer values

With a long-term load of σ_m = 20.4 MPa, the void ratio in test TK-031 reduced from e = 0.107 to e = 0.074 after t = 136 d in a range defined as representing creep compaction. The compaction rate in this instance only declined from $\dot{\varepsilon}_v$ = $2.1 \cdot 10^{-9}$ to $1.5 \cdot 10^{-9}$ s^{-1}, in other words, less than 15 % of an order of magnitude. This differs to the odometer data which indicate a decline of 3 orders of magnitude ($\dot{\varepsilon}_v$ ≈ $1 \cdot 10^{-8}$ to $1 \cdot 10^{-11}$ s^{-1}) for the comparable void ratio zone.

This therefore fails to confirm the general decline in the compaction rate under conditions where the formation pressure cannot rise any further and generally derived from odometer

test results in the residual porosity range at low temperatures. The result from TK-031 where σ_m = 20.4 MPa indicates a much more favourable material behaviour in the sense of the fastest possible compaction to give rise to an effective barrier.

3.9 Extrapolation of the compaction behaviour of TK-031

The TK-031 compaction test involved compaction under a maximum load of 20.4 MPa to give a void ratio of e = 0.074. The compaction rate at the end of the compaction lasting almost 300 d was still around $1.5 \cdot 10^{-9}$ s^{-1}. The following attempts to estimate how the compaction of the already significantly compacted test specimen would have proceeded further in the direction of rock salt quality (e ≈ 0). Because no further experimental data is available, and the dominating compaction mechanism in the test cannot be separated out to derive extrapolation formulae, the extrapolation of the compaction rate will be undertaken by using previous empirical experience from other tests in a qualitative rather than a mathematical approach.

The time-dependent visualisation of the compaction rates (Figs. 8 and 9) are not suitable for extrapolation down to rock salt density because the forecast trend of the curves is completely uncertain over long periods of time. The volumetric strain rates $\dot{\varepsilon}_v$ ("dEpsv/dt") and the compensation curves are therefore drawn in Fig. 11 as a function of the void ratio (red or black with yellow dots). The abscissa begins on the left with a void ratio of e = 0.2 (≈ initial density of sample TK-031) and ends on the right-hand side with e = 0, i.e. the calculated density of compacted rock salt. The available laboratory results confirm around two thirds of the scale up to e = 0.075. The compaction ε_v ("Epsv", blue) shows the amount of experimental time required to achieve the compaction state in each case (void ratio) with respect to the secondary axis. The test values with e_{min} = 0.075 end at t = 297 days.

The results of compaction phases 1 to 4 and compaction phase 5 up until the interruption where e = 0.107 (t = 136 d) indicate a relatively unequivocal trend. However, because they are dominated by the influences of the previous load increases, they are also unsuitable for extrapolation. As already discussed in Chapter 3.7, only the results at the end of each load phase can be considered characteristic for each stress and compaction state. The transition to the then dominating creep compaction involved in these cases is obviously associated with a change in direction of the compaction rate, as seen particularly clearly at the end of the 3rd, 4th and the 1st part of the 5th loading phase. This finding is also demonstrated by the compaction rate in the range e = 0.095 (t = 180 d) after reloading from e = 0.107 (t = 136 d). In terms of values, the transition is in the same range as before

R & D Radioactive Waste Repository
Stührenberg, D.(2013): Triaxial Compaction Test TK-031
Evaluation Report; Hannover (BGR)

Page 27 of 33

the unforeseen 2nd test interruption, but falls, together with the 3rd test interruption. It is not possible to exclude the effect of some resulting influence, although it is no longer possible to confirm this unequivocally. However, the connection between the two phases under similar load deduced from the time-dependent visualisation (Fig. 9) also appears plausible in this visualisation.
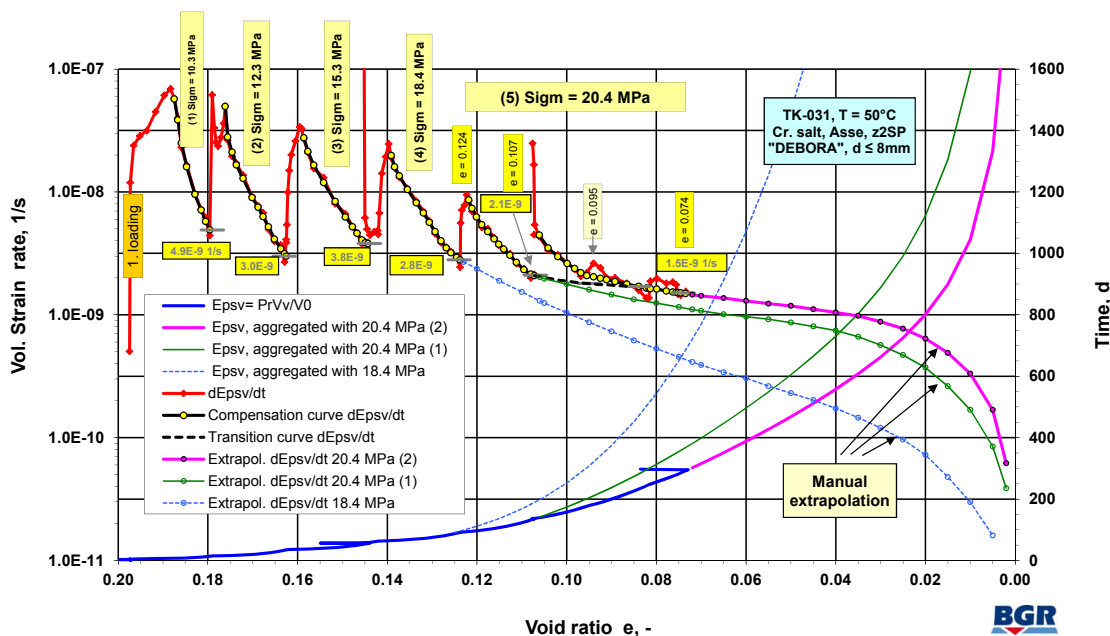

Fig. 11: Extrapolation of the compaction rates from test TK-031

In the initial approach, the extrapolation of the $\dot{\varepsilon}_v$-e plot beyond the end of the test on the 297th test day uses the compensation curve determined from approx. e = 0.095 as the basis and extrapolates it with the same trend (plot in Fig. 11: magenta, dotted). Towards the end of the compaction achieved under constant external load, the compaction rate will decrease progressively because of the ever decreasing percentage of pore space, and will asymptotically approach the value e = 0. Because of the test results achieved pursuant to Chapter 3.8, one is justified in assuming that a significant decrease under triaxial conditions would only be engendered after very high compaction even with "dry" crushed salt material. In the plot selected in Fig. 11, the compaction rate $\dot{\varepsilon}_v$ has not dropped below a value of $1 \cdot 10^{-10}$ s^{-1} until e < 0.005.

The compaction progress associated with working steps of Δe = 0.005 is calculated and aggregated from the extrapolated curve to estimate the void ratio. This results in the magenta-coloured plot shown in Fig. 11 which continues smoothly from e = 0.074 (t = 296 d) with the blue test curve. After 800 days (2.2 years) it reaches a void ratio of 0.02, and after around 5 years e = 0.002 (off the scale). It is important to note again that this extrapolation is not verified by test results.

R & D Radioactive Waste Repository
STÜHRENBERG, D.(2013): Triaxial Compaction Test TK-031
Evaluation Report; Hannover (BGR)

Page 28 of 33

To demonstrate the sensitivity with respect to the achievable crushed salt compaction, two other possible compaction rate curves are assumed and calculated. If one selects an extrapolation curve corresponding to the end of the unplanned interruption of the loading phase σ_m = 20.4 MPa at e = 0.107, in the form of the green plot, the values e = 0.02 and e = 0.002 are not reached until 3 years and 8 years respectively. The dashed light blue line represents a possible compaction over time under a constant load of σ_m = 18.4 MPa. A void ratio of e = 0.02 in this case is only calculated to occur after 11 years.

4   Summary and conclusions

The triaxial compaction test was undertaken with the aim of quantitatively determining with greater precision, as well as with respect to the stress state, the compaction behaviour of laboratory-dried crushed salt qualitatively indicated by earlier odometer tests. The residual porosity range is of particular interest because it can be assumed here that the compaction stress (formation pressure) cannot be increased further in situ and that therefore the test specimens are predominantly affected by creep compaction.

In addition to the initial state and the final state of the test specimen in an unstressed state, the crucial measurement parameter of the test is the measurement of the air volume displaced during compaction. The burette apparatus used for this purpose was re-calibrated after carrying out conversion and improvement work.

Five different quasi-hydrostatic loading phases, σ_m = 10.3; 12.3; 15.3; 18.4 and 20.4 MPa, were run for durations of 7, 19, 26, 27 and 202 days. The loading or load increase rates were between 3 MPa/d and 1 MPa/d. The transition to the next (higher) loading phase was undertaken when the obvious influence on the calculated compaction rate from the previous loading phase had dropped off or was considered to have dropped to an insignificant level. The values registered here were evaluated as characteristic for the actual stress and compaction state. The last phase with σ_m = 20.4 MPa was run as a long-term test for creep compaction. It not only provided material parameters in the residual porosity range, but also provided a good basis for extrapolation of the results beyond the end of the test period.

For technical reasons, the test had to be interrupted three times for brief depressurisation and repressurisation periods, which complicated the evaluation of the compaction behaviour particularly because of the sensitive volume measurements.

The results of an odometer test run in 1994 were used in a stress-void ratio diagram and compared with the values of the TK-031 triaxial test. The "backfill resistance" determined by the odometer tests was converted to the median stress σ_m by using an empirically

R & D Radioactive Waste Repository
Sᴛüʜʀᴇɴʙᴇʀɢ, D.(2013): Triaxial Compaction Test TK-031
Evaluation Report; Hannover (BGR)

Page 29 of 33

determined calculation approach in the ratio of axial stress to radial stress. The compaction rates from the TK-031 test at the end of the loading phases, as well as creep compaction phases, 1 to 4, lie in the σ-e-diagram above the corresponding comparative values from the odometer test and with a growing trend – in other words, more unfavourable in the sense of the fastest possible compaction. The values lying on the horizontal line σ_m = 20.4 MPa of the 5th loading phase run for more than 200 days were also initially less favourable but do not demonstrate the significant reduction in compaction rate with increasing compaction as derived from the displacement controlled odometer tests. The compaction rate in test TK-031 in the relevant void ratio range of 0.095 to 0.074 where $\dot{\varepsilon}_v$ = 2.1•10⁻⁹ to 1.5•10⁻⁹ s⁻¹ has dropped by less than 15 % of an order of magnitude.

The converted odometer results in this range where $\dot{\varepsilon}_v$ ≈ 1•10⁻⁸ to 1•10⁻¹¹ s⁻¹ cover more than 3 orders of magnitude. The TK-031 test therefore does not confirm the significant decline in the compaction rate derived from the odometer test results in the residual porosity range at low temperatures when the formation pressure can no longer increase.

Because of the two counteractive trends concerning the differences between the triaxial and odometric test results, and their range of up to 3 orders of magnitude, it is considered fairly unlikely that the primary cause involves measurement inaccuracies or simple scatter of the results.

Moreover, because there is a successively rising trend in the difference to the odometer results, for values considered to be characteristic, after the influence of the loading diminishes, and with rising stress or backfill resistance, it seems logical to check the validity of the estimation of the odometer results pursuant to equation (17).

A comparison of the results of the triaxial and the odometer compaction assumes that an unequivocal material behaviour exists for each compaction state, in other words, that the combination "displacement controlled load – backfill resistance" and "stress-regulated load – compaction rate" leads to the same results. It is not possible to exclude, however, that, despite the relatively large dimensions of the test specimens, different dominant compaction mechanisms exist because of the different geometries, the boundary conditions, and the possibly anisotropic material behaviour of crushed salt (grain shape and position of angular grains) in the different types of tests. It is feasible that horizontal grain dislocations caused by the confining pressure under triaxial load involve a lower amount of energy than the vertical compaction required in the naturally restricted odometer cells. It is not possible to clarify this situation in the context of this test.

With respect to the original objective of quantifying the results of the less complicated odometer tests with the results of the triaxial compaction tests, a qualitative basis was created with the help of the analysis of the trend curve.

R & D Radioactive Waste Repository
Stührenberg, D.(2013): Triaxial Compaction Test TK-031
Evaluation Report; Hannover (BGR)

Page 30 of 33

The results gained from the test were extrapolated beyond the compaction curve derived experimentally with the aim of estimating the material behaviour beyond the test period. Because the time-dependent visualisation of the compaction rates is uncertain, these are visualised as a function of the void ratio. The incorporated compensation curve of the loading phase with σ_m = 20.4 MPa which lasted for over 200 days was extended in line with the registered trend until the progressive drop of the compaction rate expected with increasing compaction approaches e = 0 following an asymptotic curve. The compaction increments calculated and aggregated for small time intervals produced a plausible compaction curve graph where the line reaches a void ratio of e = 0.02 after 2.2 years.

In a slightly less favourable version under the same load, it took 3 years to reach this void ratio. The extrapolation oriented to the plot corresponding to the constant load σ_m = 18.4 MPa reached a void ratio of e = 0.02 after a time of 11 years.

These estimates can be used in numerical calculations as a preliminary basis to determine the creep compaction rate expected in situ within a developing barrier made out of crushed salt. Because of the existing uncertainties associated with the extrapolation, it is still necessary to verify the barrier effect in the residual porosity range by carrying out tests under the in situ relevant conditions within this compaction range, despite the expected extensive time periods involved.

R & D Radioactive Waste Repository
Stüh_renberg, D.(2013): Triaxial Compaction Test TK-031
Evaluation Report; Hannover (BGR)

Page 31 of 33

References

Bechthold, W. et al. (1999): Backfilling and Sealing of Repositories for Radioactive Waste in Salt (BAMBUS Project). Final Report 1999 – European Commission – EUR 19124EN.

Braitsch, O. (1962): Entstehung und Stoffbestand der Salzlagerstätten, Springer-Verlag

Dohrmann, R. (2010): Mineralogische Charakterisierung der Variabilität von Asse-Salzgrus-Proben (1985 – 2008). BGR/LBEG-interner Untersuchungsbericht, B2.1/L3.8, Dez. 2010 - unveröffentlicht.

Kröhn, K.-P., Stührenberg, D., Herklotz, M., Heemann, U., Lerch, C., Xie, M. (2009): Restporosität und -permeabilität von kompaktierendem Salzgrus-Versatz; Projekt REPOPERM - Phase 1. Bericht GRS-254, GRS Braunschweig, 2009. ISBN-Nr.: 978-3-939355-29-8.

Stührenberg, D.; Zhang, Cl. (1995): Untersuchungen zum Kompaktionsverhalten von Salzgrus als Versatzmaterial für Endlagerbergwerke im Salz unter besonderer Berücksichtigung der Wechselwirkung zwischen Gebirge und Versatz. BGR-Abschlussbericht zum BMFT-Fv. Förderkennzeichen 02 E 8552 8, Archiv-Nr.: 113 259; Hannover.

Stührenberg, D. (2002): Kompaktion und Permeabilität von Salzgrus. BGR-Abschlussbericht zum BfS-Arbeitspaket 9G 21382100 (Berichtszeitraum 1998 – 2001), Tagebuch-Nr.: 11 145/2000; Hannover.

R & D Radioactive Waste Repository
STÜHRENBERG, D.(2013): Triaxial Compaction Test TK-031
Evaluation Report; Hannover (BGR)

Page 32 of 33

List of tables   Page

R & D Radioactive Waste Repository
STÜHRENBERG, D.(2013): Triaxial Compaction Test TK-031
Evaluation Report; Hannover (BGR)

Page 33 of 33

List of figures
Page